

General Disclaimer

One or more of the Following Statements may affect this Document

- This document has been reproduced from the best copy furnished by the organizational source. It is being released in the interest of making available as much information as possible.
- This document may contain data, which exceeds the sheet parameters. It was furnished in this condition by the organizational source and is the best copy available.
- This document may contain tone-on-tone or color graphs, charts and/or pictures, which have been reproduced in black and white.
- This document is paginated as submitted by the original source.
- Portions of this document are not fully legible due to the historical nature of some of the material. However, it is the best reproduction available from the original submission.

SATURNIAN KILOMETRIC RADIATION: SOURCE LOCATIONS

**M. L. Kaiser and M. D. Desch
NASA/Goddard Space Flight Center
Laboratory for Extraterrestrial Physics
Planetary Magnetospheres Branch
Greenbelt, Maryland 20771**

ABSTRACT

Using Voyager 1 and 2 Planetary Radio Astronomy data and reasonable assumptions about radiation beam geometry, we deduce the source locations of both polarization components of the Saturn kilometer-wavelength radiation. The resulting radio source footprints are compared with the surface locations of Saturn's UV aurorae, polar cap boundary, and polar cusp. Our methodology and results are contrasted with those of Lecacheux and Genova, submitted in a companion paper in this issue.

INTRODUCTION

Intense Saturnian kilometer-wavelength radio emission (SKR) has been observed by the Voyager 1 and 2 Planetary Radio Astronomy instruments [Warwick et al., 1977] since January 1980 [Kaiser et al., 1980]. Having a spectral peak near 200 kHz in the kilometer-wavelength band, the emission actually extends from about 20 to 1200 kHz. SKR shows a strong, repeatable variation in occurrence probability over a 10h 39.4m period [Desch and Kaiser, 1981]. This period was inferred to be the rotation period of Saturn's magnetic field, and the periodic variation of SKR occurrence was taken to indicate that the source region was confined in longitude and rotated with the planet. After the Voyager 1 closest approach to Saturn in November 1980, when Saturn was observed from above its night hemisphere, it was clear that the SKR source did not rotate with the planet but stayed fixed relative to the Saturn-sun line, waxing and waning in intensity with the Saturnian rotation [Warwick et al., 1981; Gurnett et al., 1981]. In other words, it appeared that when a particular small range of longitudes arrived at a particular solar hour angle the SKR maximized.

The emission was predominantly right-hand (RH) polarized as observed by both Voyager instruments inbound to Saturn. The spacecraft approached Saturn from just duskward of the Saturnian noon meridian and almost 10° north of its equator. The Voyager 1 trajectory after the November 1980 closest approach to Saturn was at approximately 3.5-hr local time and 26° north latitude. The SKR observed on this outbound trajectory was generally weaker than that observed

from the inbound leg. and was exclusively RH polarized. Left-hand (LH) polarized SKR was observed only intermittently during the inbound trajectories, but was dominant during the Voyager 1 closest approach period when the spacecraft was south of the Saturnian equator plane. Based largely on this polarization morphology, Warwick et al. [1981] inferred that SKR is emitted in the magnetoionic extraordinary (χ) mode with the RH emission originating in the Saturnian northern hemisphere and the LH emission in the in the southern hemisphere.

Kaiser et al. [1981] were able to place severe constraints on the source location of the RH polarized SKR by using these observations combined with some simple assumptions based on comparison between SKR and the earth's auroral kilometric radiation (AKR). They made three assumptions, illustrated schematically in Fig. 1, concerning the topology of the SKR radiation pattern. First, following Warwick et al. [1981], they assumed that the SKR at a given frequency is generated just above the X mode cutoff. For the case of Saturn this is very nearly the electron gyrofrequency, since the electron plasma frequency deduced from the radio occultation measurements [Tyler et al., 1981] falls off very rapidly with altitude. Second, Kaiser et al., [1981] assumed that the SKR radiation fills a very broad beam whose axis of symmetry is directed parallel (or antiparallel) to the magnetic field direction in the source region. Finally, they assumed that the SKR radiation pattern drops to insignificant levels at 90° or more from the beam axis. In other words, the beam front-lobe-to-back-lobe ratio is very large. They actually used three beam shapes in their study, each with a power pattern which fell off with angle (i) from the beam axis according to a $\cos^2 i$, $\cos i$ or $\cos^{1/2} i$ law. They found that the results were insensitive to the details of the beam pattern assumed, provided that the cutoff at $i = 90^\circ$ existed.

These three assumptions appear to be on very good grounds. For example, Benson and Calvert [1979] first showed that the earth's AKR is generated just above the X mode cutoff. Also, several studies [Alexander and Kaiser, 1976; Green et al., 1977; Gallagher and Gurnett, 1979] showed conclusively that AKR is emitted into a broad lobe. In particular, Figure 6 of Green et al. [1977] indicates that, near the spectral peak of AKR, the emitted beam falls off like a cosine relative to the center of the beam. Green et al. [1977] and

Alexander and Kaiser [1976] both showed that the front-lobe-to-back-lobe ratio for AKR is very large, on the order of 1000 to 1, and, recently, Calvert [1981 a,b] has shown that the AKR beam pattern is oriented such that its axis is approximately parallel to the magnetic field direction.

Having adopted these assumptions, Kaiser et al. [1981] solved for the emission locations, in latitude and local time around Saturn, necessary to yield the observed change in average SKR intensity with changing Voyager 1 viewing geometry. Specifically, they searched for source locations where the SKR beam depicted above would simultaneously illuminate both the inbound and outbound trajectories of Voyager 1, but where the observed power flux on the inbound leg would exceed that on the outbound leg by a specified amount. The resulting source locations were then traced down their respective magnetic field lines (centered, axially aligned dipole) to the 'surface' of Saturn to produce the rather broad footprint of the RH source shown in Fig. 1. Sources on any or all of the field lines whose footprints are inside the blackened area satisfy the Voyager 1 inbound to outbound average flux ratio criteria. The footprint shown in Fig. 1 is for 175 kHz, near the frequency of maximum flux for SKR [Kaiser et al., 1981]. Footprints for other SKR frequencies generally intersect the 175 kHz footprint at latitudes above about 60°.

Since no LH polarized emission was ever observed on the outbound leg of Voyager 1, no estimate of the LH source location could be made until now. In this paper we take advantage of the Voyager 2 observations that provide a different viewing geometry from that of Voyager 1 and that include a large amount of LH polarized emission data. We use these data in the context of the three assumptions already described to locate the footprint of the LH polarized source and to further constrain the RH source footprint. We then discuss the implications of the resulting SKR source locations and compare them with observations from other Voyager instruments.

RESULTS

In order to locate the LH polarized source, we have combined data from 1) the Voyager 1 inbound pass, during which time a small but significant amount of LH emission was detected and 2) the Voyager 2 closest approach interval and

subsequent outbound leg, when we observed LH emission exclusively [Warwick et al., 1982]. The trajectories in equator and meridian plane projection for these times are shown in Fig. 2a and 2b, where the heavy bars on the spacecraft trajectories indicate schematically where the relevant observing intervals occurred. Spacecraft local time and latitude relative to Saturn were nearly constant at these times. The viewing geometry at closest approach, indicated by a small filled square in the figure, was centered at about 0.6 hr local time and -14° latitude. Adopting the beam shape and alignment assumptions outlined above, two families of footprint solutions are found, depending on inbound to outbound average flux ratios. Since final processing of the Voyager 2 data is incomplete, one additional observation (described below) allows us to exclude one of the two possibilities, namely, inbound flux $>$ outbound flux. If this flux ratio existed, the source footprint would be inside the dashed region shown in Fig. 2c; however, if the converse is true, the darkly-shaded region must contain the source field line(s). Like Fig. 1, Fig. 2c also shows the 175 kHz footprint. Other frequencies have very similarly oriented footprints.

The Voyager 2 observations near the time of closest approach provide information that further constrain the northern- and southern-hemisphere source locations (and, hence, the inbound/outbound flux ratio for LH emission). Fig. 3a shows the Voyager 2 PRA polarization observations in dynamic spectrogram format for the 37-hour interval approximately centered on closest approach (C.A.). Light shading represents RH emission, black represents LH emission, and no shading indicates no emission. For the hours and indeed months before closest approach, the emission was almost exclusively RH, whereas LH was the predominant polarization after closest approach. Since the Voyager 2 inbound trajectory was at northern latitudes and the outbound trajectory was at southern latitudes, this observed change in polarization is consistent with our previous result that the RH emission is generated at high latitudes in the northern hemisphere, and LH emission is from a comparable region in the southern hemisphere [Kaiser et al., 1981; Warwick et al., 1982]. For the 4-hour period near Voyager 2 closest approach, no SKR from either hemisphere was detected. Fig. 3b shows the view of Saturn from Voyager 2 for the period before, during, and after closest approach. The northern hemisphere source region that was deduced from the Voyager 1 observations

[Kaiser et al., 1981] is easily in 'view' before closest approach, but by the time of closest approach, only sources mapping to the small region shown in the center panel of Fig. 3b still illuminate the spacecraft. In other words, although the actual point of emission may have been 'visible' to the spacecraft, the emission beam was oriented toward the dayside hemisphere so that Voyager 2 was more than 90° from the line of sight. After closest approach, the northern hemisphere source never again illuminates the observer, but the southern hemisphere source region is easily viewed. Therefore, we interpret the SKR disappearance near closest approach as indicating that Voyager 2 was out of the radiation beam of both the northern and southern SKR sources for that interval of time.

We have examined the frequency dependence of our results by measuring the flux ratios at numerous locations across the 20 to 1200 kHz SKR band and projecting the resulting source locations down to the surface. We find only insignificant shifts in the source footprints as the frequency is varied. Of course, the altitude of the source region on a given magnetic field line depends strongly on frequency as required by our first assumption, but the surface locations remain fixed. This same conclusion applies to the disappearance/reappearance phenomenon, which was not observed to be strongly dependent on frequency. This observation is entirely consistent with the model assumptions we have adopted because, relative to both the RH and LH emission beams, the observer reaches the point at which he is 90° off beam axis at nearly the same time at all frequencies.

Our best estimates of the RH and LH source locations are shown in Fig. 4. Here we have made use of three sets of footprints for each hemisphere. For the north, we have the footprints derived from comparison of the trajectory pairs of Voyager 1 inbound and Voyager 1 outbound, Voyager 1 (or 2) inbound and RH disappearance at Voyager 2 closest approach, and, Voyager 1 outbound compared with RH disappearance. For the southern hemisphere, the three pairs are, Voyager 1 inbound and Voyager 2 outbound, LH reappearance at Voyager 2 closest approach compared with both Voyager 1 inbound and Voyager 2 outbound. By noting the intersection of all solutions, that is, the area held in common by all footprints, we derive the results shown in the figure. We find that the northern hemisphere SKR source footprint is restricted to the small

triangular area near 11-hr local time and 75° latitude. It is only from field lines emanating from this region that RH SKR is more intense viewed from Voyager 1 inbound vs outbound and disappears at the correct time near Voyager 2 closest approach. For the southern hemisphere, only the source locations that map to the thin line shown in Fig. 4 can both be observed by Voyager 1 inbound and Voyager 2 outbound and also come into view by Voyager 2 at the time shown in Fig. 3. The results shown in Fig. 4 are, again, for 175 kHz, but we have found that virtually all SKR frequencies will reproduce essentially the same source footprints. Thus, our findings indicate that all SKR can originate from the same field line or group of field lines, just like the AKR [Alexander and Kaiser, 1976].

DISCUSSION

We ultimately wish to relate the source footprint local times to the longitude system on Saturn (SLS) that corotates with the planet [Desch and Kaiser, 1961]. This would be valuable, for example, in relating the radio emission sources to phenomena that are associated with a particular range of longitudes. To establish a local time-SLS relationship, we note that the occurrence probability of the RH and LH SKR are a maximum when a particular longitude is on the noon meridian. Thus the RH SKR has a maximum occurrence probability when 100° SLS is on the noon meridian, and the LH SKR maximizes when 0° SLS (approximately) is on the noon meridian. This means that the northern SKR footprint must be confined to an area on the planet near 115° SLS (100° plus the difference in degrees between the noon meridian and the footprint local time). In similar fashion we confine the southern SKR footprint to about $0^\circ < \text{SLS} < 70^\circ$. Thus, by virtue of their localization in longitude and latitude, these sources may be dynamically related to other important phenomena and field topologies near Saturn's surface. For example, Voyager 2 measurements of the auroral brightness [Sandel et al., 1962] also indicated a localized 'active' region, and the derived position agrees in latitude, longitude and local time with the northern SKR source footprint shown in Fig. 4. Similar Voyager 1 measurements [Broadfoot et al., 1961] indicated a high latitude 'active' region in the southern hemisphere in the same longitude range as the SKR southern footprint shown in Fig. 4. With regard to Saturn's main magnetic field, Behannon et al. [1961], using a

realistic magnetotail current system, modeled a Saturnian polar cap boundary and polar cusp near 10° colatitude in both hemispheres. Thus, the localization of the RH SKR source near the noon meridian and about 10° colatitude is suggestive of an association with the dayside polar cusps. The earth, too, is observed to have a kilometer-wavelength radio component associated with its dayside cusp region [Alexander and Kaiser, 1977]. Although this component is decidedly weaker than the nightside AKR source, it may be the analog of Saturn's radio emission.

We see that several independent lines of evidence are now pointing toward some irregularity in Saturn's high latitude regions, probably near 115° SLS based on the RH SKR, and possibly at other longitudes, based on the LH SKR. Because of the strong rotational modulation of SKR and the lack of significant magnetic field tilt [Ness et al., 1981] to explain it, Kaiser et al. [1980] had suggested that this irregularity might correspond to an anomaly in Saturn's near-surface magnetic field. Direct measurement of such a departure from a simple dipole configuration is difficult in this case, however, because the spacecraft, except when it was at very large distances from the planet, never sampled field lines that map down to the SKR footprints. Lacking direct confirmation, we suggest that there is indirect evidence of small near-surface departures from dipole-like fields at high latitudes on Saturn.

We now have a reasonably complete picture of the source location geometries for Saturn and, of course, for the earth. We might speculate, then, as to why the two planets have sources in opposite hemispheres, nightside for earth and dayside for Saturn. It is well known that magnetotail dynamics and associated substorm activity are important terrestrial processes, and AKR is certainly a related phenomenon [Kaiser and Alexander, 1977 and references therein]. The lack of any nightside radio source on Saturn might then imply that magnetotail processes are less important there, perhaps due to the relative dominance of convection versus rotation dynamics in the two planets' magnetospheres. The fact that the earth also has a weak dayside source, as we mentioned above, suggests that this convection/rotation dichotomy is not complete; however, the total absence of any nightside Saturn radio source certainly implies that the role that convection might play for that planet is diminished, at least in the context of auroral radio emissions.

In a companion paper, Lecacheux and Genova [1982] also study the problem of determining the SKR source location. They have made two assumptions which differ greatly from those used in our analysis: 1) SKR is emitted isotropically from an unspecified altitude, and 2) the disappearance/reappearance of SKR (e.g., Fig. 3) is due entirely to physical occultation of the source region by Saturn. They derive a source footprint that, in the northern hemisphere, overlaps (barely) our source location shown in Fig. 4, and, hence, is consistent with the auroral bright spot deduced by Sandel et al. [1982]. Their southern source footprint, however, does not overlap with that shown in Fig. 4, and also does not intersect the southern auroral zone determined by Broadfoot et al. [1961]. Much more serious, however, is the fact that in order to explain the observations using their assumptions, Lecacheux and Genova require that the source altitude must be approximately the same for all frequencies (20 to 1200 kHz), and be near zero, i.e., near the cloud tops. This restriction on source altitude presents a number of problems concerning the possible emission mechanism for SKR. Near the cloud tops, most if not all of the SKR frequency range would be below the cutoff frequency for X mode emission. This would require that SKR either be generated in the ordinary (O) mode near the local electron plasma frequency in order to escape at all, or be generated in the X mode below the cutoff and subsequently 'tunnel' through the stop band to free space. However, if SKR is O mode emission, the polarization would be opposite to that actually observed. On the other hand, it is not clear by what mechanism X-mode emission could be generated over the observed frequency band from a very restricted range of altitudes. And even if the emission could be so generated, it could not reach free space without being greatly attenuated. We conclude that our analysis, which rests on plausible assumptions that are manifestly consistent with present understanding of the earth's radio emission, lends greater credence to the source locations deduced.

ACKNOWLEDGMENTS

We are indebted to Fred Espenak for developing the three dimensional global projection routines, and to J. K. Alexander and T. J. Birmingham for many valuable suggestions and discussions.

REFERENCES

- Alexander, J. K. and M. L. Kaiser, Terrestrial kilometric radiation: Spatial structure studies, J. Geophys. Res., 81, 5948-5956, 1976.
- Alexander, J. K. and M. L. Kaiser, Terrestrial kilometric radiation: Emission from the magnetospheric cusp and dayside magnetosheath, J. Geophys. Res., 82, 98-104, 1977.
- Behannon, K. W., J. E. P. Connerney, and M. F. Ness, Saturn's magnetic tail: Structure and dynamics, Nature, 292, 753-755, 1981.
- Benson, R. F. and W. Calvert, ISIS-1 observations at the source of the auroral kilometric radiation, Geophys. Res. Lett., 6, 479-482, 1979.
- Broadfoot, A. L., B. R. Sandel, D. E. Shemansky, J. B. Holberg, G. R. Smith, D. F. Strobel, J. C. McConnell, S. Kumar, D. M. Hunten, S. K. Atreya, T. M. Donahue, H. W. Moos, J. L. Bertaux, J. E. Blamont, R. B. Pomphrey, and S. Linick, Extreme ultraviolet observations from Voyager 1 encounter with Saturn, Science, 212, 206-211, 1981.
- Calvert, W., The signature of auroral kilometric radiation on ISIS 1 ionograms, J. Geophys. Res., 86, 76-82, 1981a.
- Calvert, W., The AKR emission cone at low frequencies, Geophys. Res. Lett., in press, 1981b.
- Desch, M. D., and M. L. Kaiser, Voyager measurement of the rotation period of Saturn's magnetic field, Geophys. Res. Lett., 8, 233-256, 1981.
- Gallagher, D. L. and D. A. Gurnett, Auroral kilometric radiation: Time-averaged source location, J. Geophys. Res., 84, 6501-6509, 1979.
- Green, J. L., D. A. Gurnett and S. D. Shawhan, The angular distribution of auroral kilometric radiation, J. Geophys. Res., 82, 1825-1836, 1977.

Gurnett, D. A., W. S. Kurth and F. L. Scarf, Plasma waves near Saturn: Initial results from Voyager 1, Science, 212, 235-239, 1981.

Kaiser, M. L. and J. B. Alexander, Relationship between auroral substorms and the occurrence of terrestrial kilometric radiation, J. Geophys. Res., 62, 5263-5286, 1977.

Kaiser, M. L., M. D. Desch, J. W. Warwick, and J. B. Pearce, Voyager detection of nonthermal radio emission from Saturn, Science, 209, 1238-1240, 1980.

Kaiser, M. L., M. D. Desch and A. Lecacheux, Saturnian kilometric radiation: Statistical properties and beam geometry, Nature, 292, 731-733, 1981.

Lecacheux, A., and F. Genova, Localization of the source of Saturn's kilometer wave radio emission, Geophys. Res. Lett., this issue, 1982.

Ness, N. F., M. H. Acuna, R. P. Lepping, J. E. P. Connerney, K. W. Behannon, L. F. Burlaga, and F. M. Neubauer, Magnetic field studies by Voyager 1: Preliminary results at Saturn, Science, 212, 211-217, 1981.

Sandel, B. R., D. E. Shemansky, A. L. Broadfoot, J. B. Holberg, G. R. Smith, J. C. McConnell, D. F. Strobel, S. K. Atreya, T. M. Donahue, R. W. Moos, D. M. Hunten, R. B. Pomphrey, and S. Linick, Extreme ultraviolet observations from Voyager 2 encounter with Saturn, Science, in press, 1982.

Tyler, G. L., V. R. Eshleman, J. D. Anderson, G. S. Levy, G. F. Lindal, G. E. Wood and T. A. Croft, Radio science investigation of the Saturn system with Voyager 1: Preliminary results, Science, 212, 201-206, 1981.

Warwick, J. W., J. B. Pearce, R. G. Peltzer, and A. C. Riddle, Planetary radio astronomy experiment for the Voyager missions, Space Sci. Rev., 21, 309-319, 1977.

Warwick, J. W., J. B. Pearce, D. R. Evans, T. D. Carr, J. J. Schauble, J. K. Alexander, M. L. Kaiser, M. D. Desch, B. M. Pedersen, A. Lecacheux, G.

Daigne, A. Boischot and C. h. Barrow, Planetary radio astronomy observations from Voyager 1 near Saturn, Science, 212, 239-243, 1981.

Warwick, J. W., D. R. Evans, J. H. Romig, J. K. Alexander, M. D. Lesch, M. L. Kaiser, M. Aubier, Y. Leblanc, A. Lecacheux, and B. M. Pedersen, Planetary radio astronomy observations from Voyager 2 near Saturn, Science, in press, 1982.

FIGURE CAPTIONS

Figure 1. An illustration of the SKR beam shape and orientation used. The emission originates along a given field line at the electron gyrofrequency corresponding, in this example, to 175 kHz. The emission is beamed into a broad three-dimensional pattern (cosine pattern shown here) with its axis of symmetry parallel to the field line at the emission point. Those source positions satisfying certain viewing criteria are mapped along their field lines to the surface ($R_S = 1$) resulting in a 'footprint' of all candidate field lines shown by the blackened area.

Figure 2a. An equator plane projection showing the local time of the Voyager 1 inbound and Voyager 2 outbound trajectories. The darkened bars along the trajectories indicate schematically where the observations were made. Also shown on the Voyager 2 trajectory is the small region near the planet from which no SKR was detected. (2b) The same as Fig. 2a, but in a meridian plane projection to emphasize the latitude of the two trajectories. (2c) The darkened area is the footprint of source field lines visible from both trajectories shown in Fig. 2a and b, and with the SKR average flux level larger viewed by Voyager 2. The other possibility, that the average flux is larger viewed by Voyager 1, would imply a source footprint inside the dashed area. However, this possibility is geometrically ruled out by the observations near closest approach.

Figure 3. The top panel shows, in a frequency-time spectrogram, the observed sense of SKR polarization for 37-hr interval centered on the closest approach. Light shading indicates RH polarization, black indicates LH polarization, and no shading indicates (in this case) no emission. The change in polarization results from the trajectory change from a northern hemisphere approach to a southern hemisphere departure. The emission gap is a consequence of the observer's viewing angle which is more than 90° from the emission beam axis of both the northern and southern hemisphere source regions. The bottom panels show the view of Saturn from Voyager 2 at the approximate times indicated with the previously deduced northern

hemisphere source region and the southern source region from Fig. 2c shown.

Figure 4. The best estimates for the source footprints of the SKR are shown. The RH emission comes from a very small area in the northern hemisphere, and the LH emission is constrained to field lines mapping to a very narrow, long band at high southern latitudes.

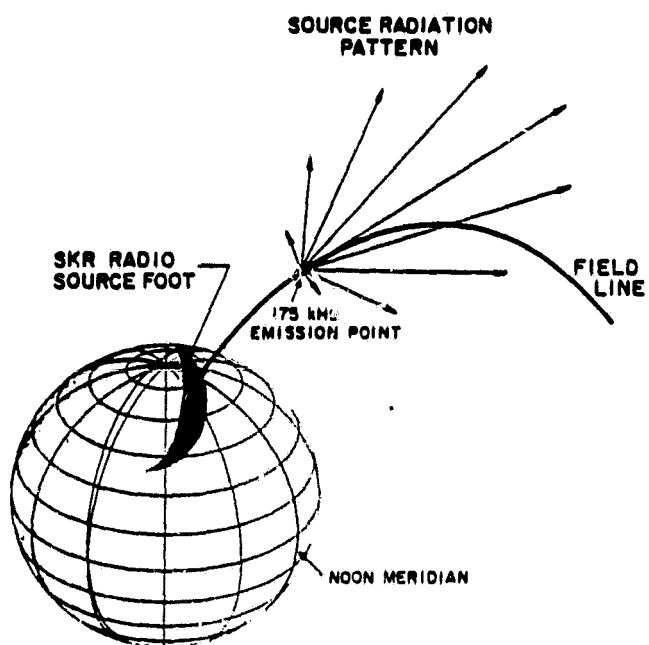


Figure 1

SOUTHERN HEMISPHERE SOLUTIONS

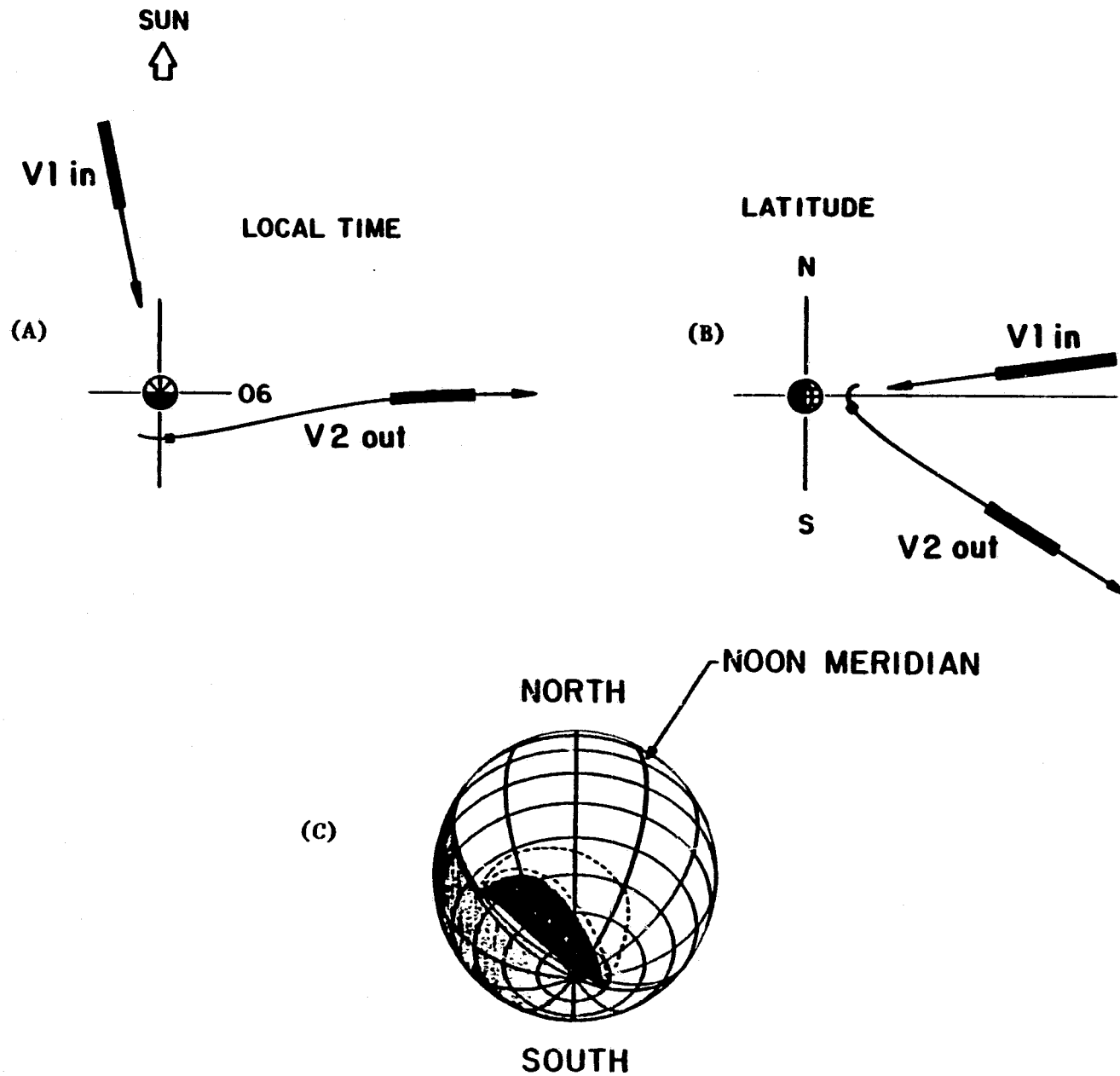
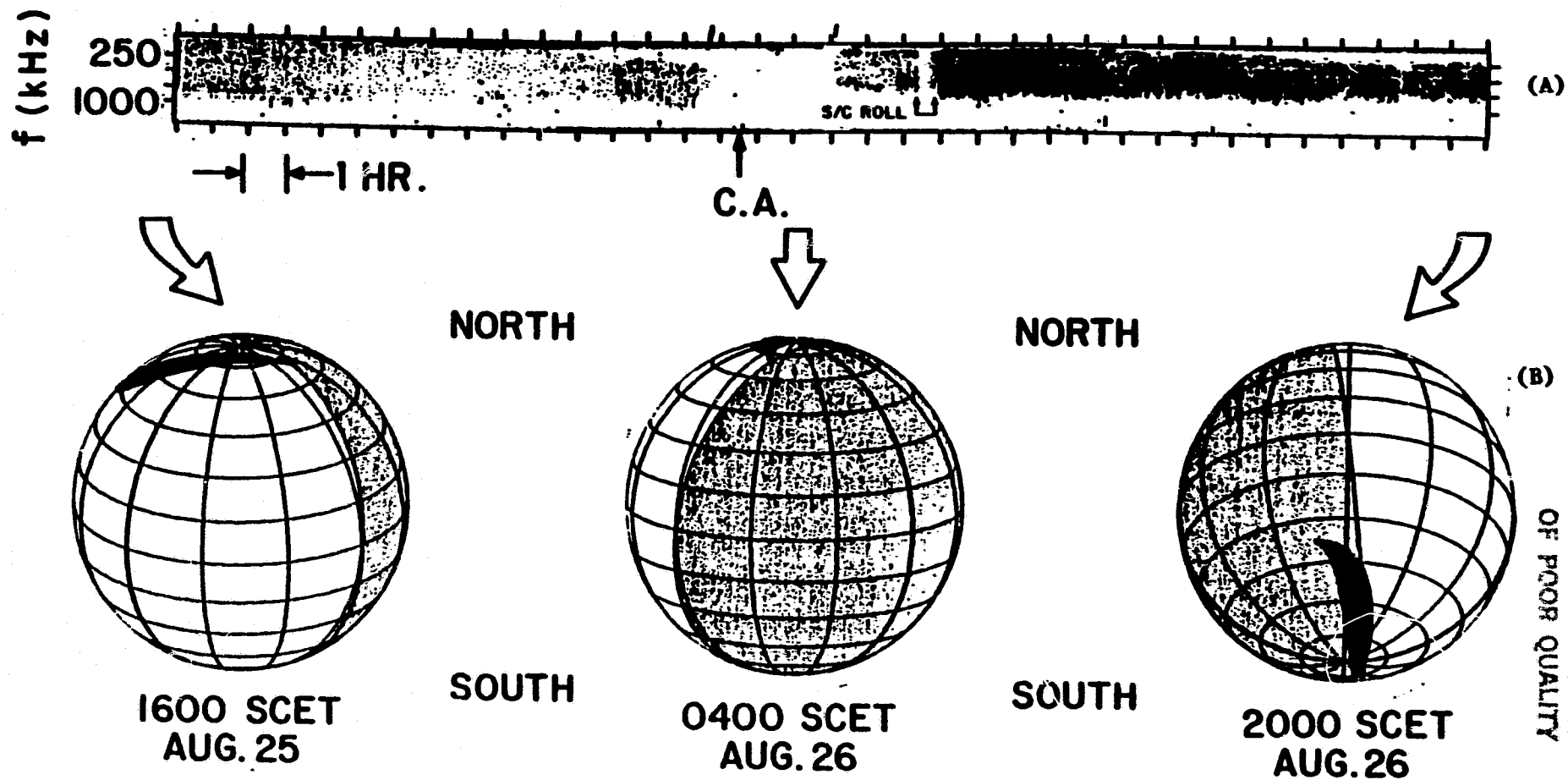


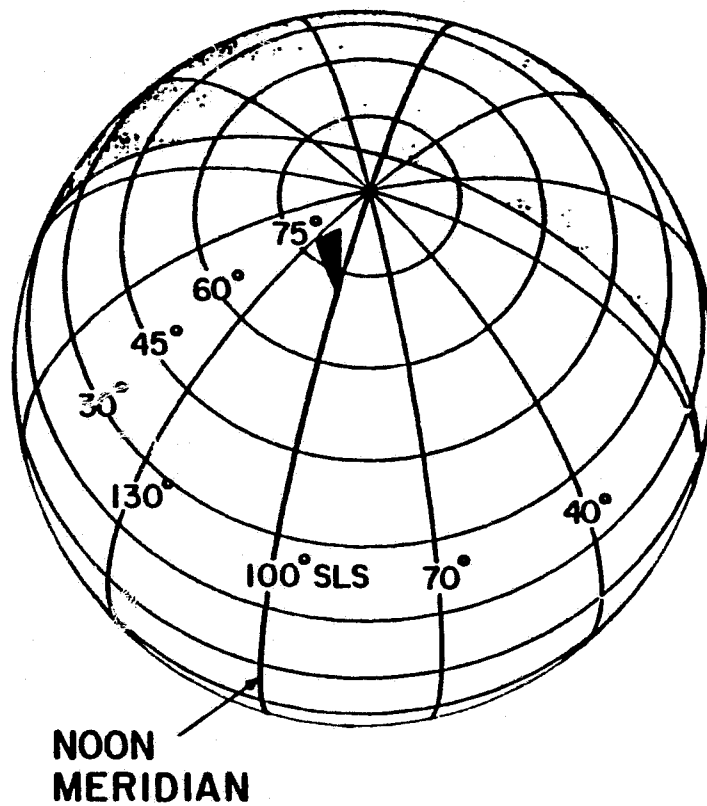
Figure 2



ORIGINAL PAGE IS
OF POOR QUALITY

SATURN'S RADIO SOURCES AS VIEWED BY VOYAGER 2

NORTHERN HEMISPHERE SOLUTION



SOUTHERN HEMISPHERE SOLUTION

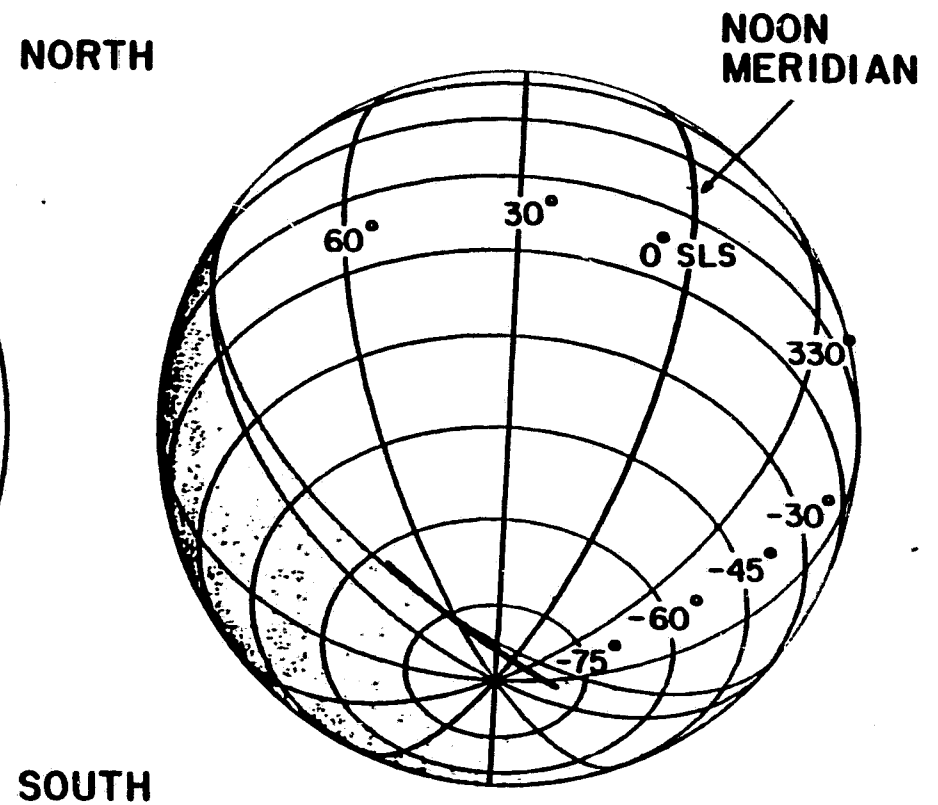


Figure 4